Title

Role of inflammation in mediating effects of dim light at night in Cntnap2 KO mouse model of autism

Author

Khosravi, Shirin

Publication Date

2024

Peer reviewed|Thesis/dissertation

UNIVERSITY OF CALIFORNIA

Los Angeles

Role of inflammation in mediating effects of dim light at night in *Cntnap2* KO mouse model of autism

A thesis submitted in partial satisfaction
of the requirements for the degree
Master of Science in Physiological Science

by

Shirin Khosravi

2024

ABSTRACT OF THE THESIS

Role of inflammation in
mediating effects of dim light at night
in *Cntnap2* KO mouse model of autism

Dr. Christopher S. Colwell, Co-Chair
Dr. Gene D. Block, Co-Chair

by

Shirin Khosravi
Master of Science in Physiological Science
University of California, Los Angeles, 2024

Nighttime light pollution is linked to metabolic and cognitive dysfunction. Many patients with autism spectrum disorders (ASD) show disturbances in their sleep/wake cycle and may be particularly vulnerable to the impact of circadian disruptors. We have previously shown that a 2-weeks exposure to dim light at night (DLaN, 5lx) disrupts diurnal rhythms and increases repetitive behaviors in contactin-associated protein-like 2 knock out (*Cntnap2* KO) mouse model of autism. In addition, we found that short wavelength enriched DLaN triggered cFos expression in the basolateral amygdala (BLA) raising the possibility that these cell populations may mediate the effects. Preliminary results revealed that DLaN increased the number of microglia, the brain resident immune cells that trigger inflammation. In this thesis, we examined the impact of exposure to DLaN on microglial density in the BLA and prefrontal cortex (PFC) of *Cntnap2* mutant mice using Ionized Calcium Binding Adaptor Molecule 1 (Iba1) as a microglial molecular

marker. 2-weeks daily treatment with DLaN evoked a mild increase in the number of Iba1+ cell in the BLA region. DLaN treatment of *Cntnap2* KO mice increased microglia immunoreactivity in the PFC region. In addition, alterations in microglia evoked by DLaN were not specific to mutants as effects were also seen in WT mice. My data indicates that microglia may mediate the deleterious effects of circadian rhythm disruption by nighttime exposure to light in the *Cntnap2* mouse model of autism. These findings suggest that circadian disruptors such as light at night should be considered in the management of ASD. Broadly, our findings are consistent with the recommendation that less exposure to light at night should be considered to optimize health in neurotypical as well as vulnerable populations.

The thesis of Shirin Khosravi is approved.

Christina A. Ghiani

Ketema Paul

Gene D. Block, Committee Co-Chair

Christopher S. Colwell, Committee Co-Chair

University of California, Los Angeles

2024

To my mom and dad . . . whose love has always been the light in my life. Thank you for nurturing me with care and affection and never giving up on me.

TABLE OF CONTENTS

LIST OF FIGURES

ACKNOWLEDGMENTS

I would like to express my deepest appreciation to my advisors, Dr. Christopher Colwell and Dr. Cristina Ghiani whose unwavering patience, and support have immensely helped me grow as a researcher. They are the wisest and kindest mentors I have known. I was touched by their enthusiasm and kindness on my very first day in the lab. I fall short of words to express my sincerest gratitude towards Dr. Cowell for the countless support and faith he has placed in my abilities and the opportunity he has afforded me. His insights, encouragement, and positive energy have fueled my determination and inspired me to push beyond my perceived limitations and I can't thank him enough.

I am incredibly grateful to my thesis committee, Dr. Gene Block and Dr. Katema Paul. Your invaluable feedback and insights as leaders have immensely assisted me with my research.

I am also grateful that I had the opportunity to meet many different people in Colwell lab. Thank you, my fellow graduate students and undergraduates, for all the help, smiles, and stories.

I would like to express my heartfelt thanks to my dearest friend, Mohammad Shahili for guiding me in writing my master's thesis. I'm grateful for your wisdom and advice Mohammad. Your words have helped me make important decisions and navigate through life's challenges. There is nothing on this earth more precious than a true friendship. Thank you for being a true, loyal friend.

CHAPTER 1

Introduction

1.1 Circadian rhythm

Circadian cycles are rhythmic changes in the physiology and behavior of almost all species regulated but not generated by the cycle of light and dark. These rhythmic changes originate from an intrinsic timekeeping system or ”biological clock” with a period of approximately 24 hours. The biological clock is synchronized by the environmental light cycle and this synchrony sets the biological clock's period to exactly 24 hours and sets the “clock” to local time. This synchrony between internal time and external time helps ensure survival and well-being. The light/dark cycle serves as the main Zeitgeber, a time cue capable of entraining the circadian rhythms. Light has a major influence on the circadian rhythm. [42] The suprachiasmatic nuclei (SCN) of the hypothalamus serve as the master circadian pacemaker. The SCN regulates circadian rhythms through a network of transcriptional–translational feedback loops that result in the rhythmic expression of clock genes. [2] A small fraction of retinal ganglion cells (RGCs) are intrinsically photosensitive retinal ganglion cells (ipRGCs) that project directly onto the SCN promoting the photic entrainment of the circadian rhythm.[3]

1.1.1 The molecular clock

The 2017 Nobel Prize in Physiology or Medicine awarded to Jeffrey C. Hall, Michael Rosbash, and Michael W. Young for the discovery of the molecular mechanisms controlling circadian rhythms in Drosophila and highlights how genetics govern complex behavior. The

circadian timekeeping system in the mammalian SCN, brain regions, and peripheral organs involves three core self-sustaining transcriptional-translational feedback loops. At dawn, (circadian time (CT) 0), CLOCK, (circadian locomotor output cycles protein kaput), and BMAL1 (brain and muscle ARNT-like 1), which are the positive regulator of the loop, heterodimerize and trigger expression of the Period (PER) 1 and 2 and cryptochrome (CRY)1 and 2 genes through interaction with E-BOX (enhancer box) regulatory sequences. The two resulting proteins PER and CRY function as the negative regulators of the loop. At dusk, PER–CRY proteins accumulate in the cytoplasm and form the PER/CRY heterodimer complex, which translocate back to the nucleus to downregulate their own expression by repressing transcriptional activity of the complex CLOCK:BMAL1. Thus, from dusk (CT12) to CT24, transcription of PER and CRY diminishes and drives degradation of PER–CRY complex and allows for a new 24-hour cycle to re-initiate. [17, 29] **(Fig.1.1)**

In a second feedback loop, which acts to keep the cycle in a steady state, the complex CLOCK:BMAL1 promotes E-box-mediated expression of the nuclear receptors (α,β,γ) retinoid acid related orphan receptor (ROR) and REV-ERB (α,β), which upon translocation into the nucleus, bind to the ROR response elements (ROREs) on the promoter region of BMAL1. RORE is BMAL1 activator, whereas REV-ERB functions to suppress transcription of BMAL1. [17, 7] **(Fig. 1.1)**.

In the third accessory loop, D-box binding protein (DBP), a transcriptional activator, and nuclear factor interleukin 3 (NFIL3) interactively regulate the expression of DNA cis-element, D-box, and PER genes. DBP up-regulates D-box and *PER* transcription and NFIL3 down-regulates these genes. Additionally, E-box regulates the expression of DBP, and NFIL3 expression is mediated by ROREs.

In addition to these tripartite interlocking feedback loop systems, the circadian molecular clock is regulated by kinases and phosphatases as well as epigenetic codes and histone modifications that modulate the precision and function of the molecular clock. [7] **(Fig. 1.1)**

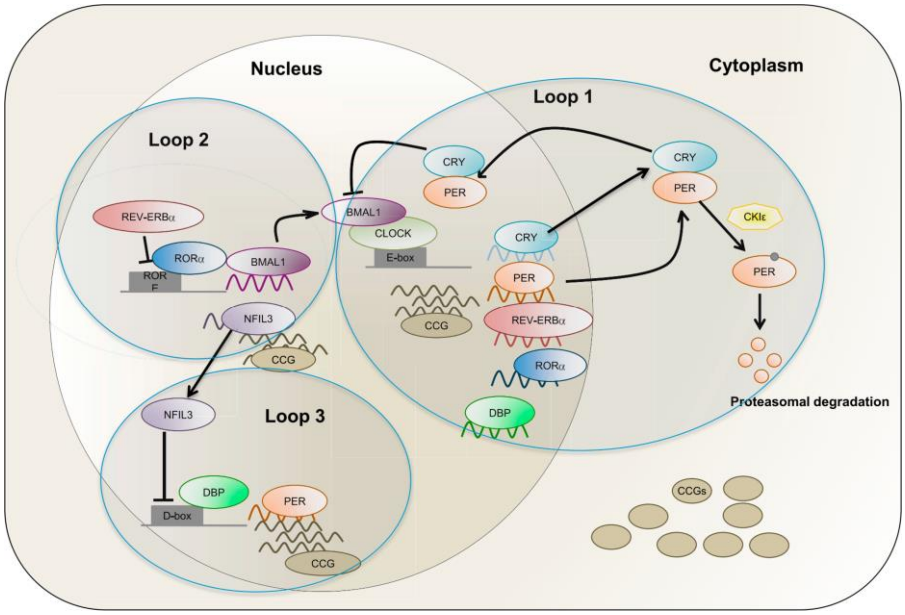

Figure 1.1: The molecular clock consists of three core interlocking feedback loops. Loop 1 contains the core clock proteins BMAL1 and CLOCK acting on E-box elements within the genes encoding the repressor proteins PER, CRY, REV-ERBa RORa, and DBP. Loop 2 involves the alternate regulation by REV-ERBa and RORa on RORE promoter elements, Bmal1 and NfIL3. Loop 3 incorporates the regulation by NFIL3 and DBP on D-box promoter elements. [7]

1.1.2 Photic entrainment of circadian rhythm; part 1: circadian photoreception

Photic entrainment of the circadian rhythm is the process by which light synchronizes the SCN internal oscillator. This process starts in the retina and involves a small population of melanopsin-containing ipRGCs with an absorption peak of 470–480 nm that send direct axonal projections to the SCN. The surprising aspect of this circuit is its independence from ordinary phototransduction by retinal photoreceptors, rods, and cones. [3] In mammals, Melanopsin, a protein found in the ipRGC type 1 (M1) cells generates retinohypothalamic tract (RHT). However, studies on melanopsin knock-out mice revealed that this photopig-

ment is only sufficient but not necessary for photic entrainment. Upon photic excitation, melanopsin-containing ipRGCs release pituitary adenyl cyclase-activating peptide (PACAP) and glutamate that binds to both N-methyl-d-aspartate (NMDA) and non-NMDA receptors and a variety of intracellular signaling molecules including but not limited to Ca2+, nitric oxide, calmodulin/calmodulin kinase, as well as immediate early-response genes such as c-fos. The neurotransmitters released by the ipRGCs by binding to receptors on the retinorecipient neuron within the ventral SCN elicit a receptor-mediated phase shift of the oscillator in the SCN. [17, 31, 34, 33] **(Fig. 1.2)**

1.1.3 Photic entrainment of circadian rhythms; part 2: SCN phase shift and output

The SCN is composed of two distinct sub-regions; a ventrolateral (VL) core and a dorsomedial (DM) shell region surrounding the core. The vasoactive intestinal polypeptide (VIP) neuronal population of the core receives photic information through the retinohypothalamic circuit and harmonically promotes expression of PER1 and PER2 in both the core and shell by binding to VPAC2 receptors. VIP neurons are the key players in resetting to light and maintaining the rhythmicity of the SCN by inducing synchronization of the VL core functions. In the shell, arginine vasopressin (AVP) neurons are co-expressed with GABA (gamma-aminobutyric acid), function as inter-neuronal coupling, and provide an output signal for synchronizing daily rhythms. [25, 41] AVP neurons also synchronize the hypothalamic–pituitary–adrenal (HPA) axis to photic cues by providing a negative feedback control over the secretion of glucocorticoids (GCs). AVP inhibits corticotrophin-releasing hormone (CRH) and assists with GCs peak production at the beginning of the active phase to ensure rhythmic regulation of HPA hormones. [25]

In addition to its role as a primary circadian pacemaker, the SCN also serves as a relay point capable of transferring its circadian phase information to the rest of the body through output pathways including the raphe-hypothalamic tract (raphe-HT) and the pineal gland-

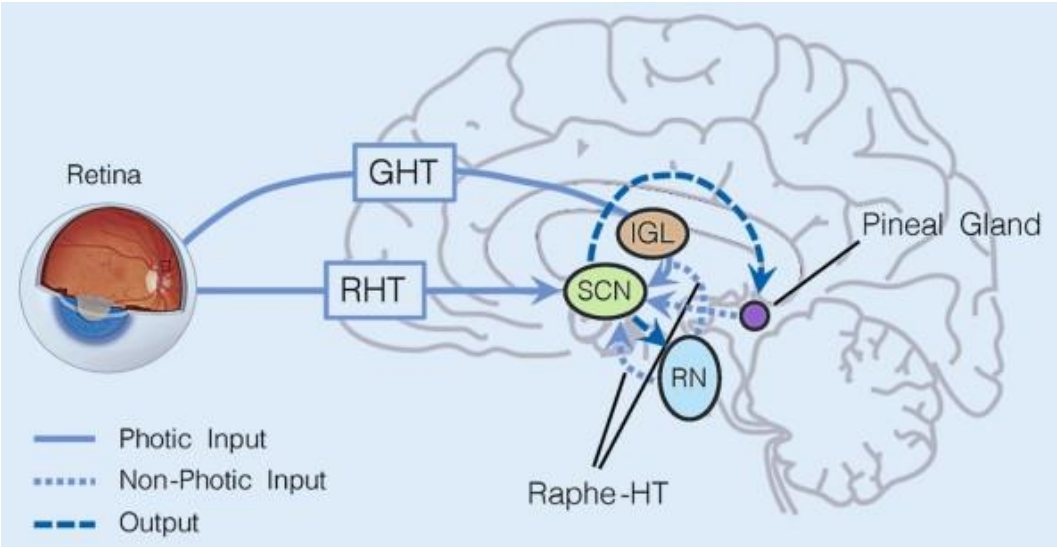

Figure 1.2: Photic input to the SCN and output pathways from the SCN. The retina relays information about the intensity of ambient light to the SCN through the retino-hypothalamic tract (RHT). The SCN receives non-photic information from the raphe nuclei (RN) via the raphe-hypothalamic tract (raphe-HT) and from the pineal gland and sends information about the phase of the circadian clock and alertness state of the body to the serotonergic RN and the pineal gland.

SCN pathway. One of the several main outputs of the SCN is to the serotonergic raphe nuclei (RN) which relay information about the circadian phase to the RN, which in turn modifies the body alertness state by sending serotonin projections to the hypothalamus and the cortex. The SCN projections to the pineal gland, where melatonin, the sleep hormone is produced and released, alter the diurnal variations between sleep and wakefulness. [5] **(Fig. 1.2)**

1.2 Autism Spectrum Disorder

Autism spectrum disorder (ASD) is a heterogeneous neurodevelopmental disease highly heritable and according to the 2010 Global Burden of Disease study is more common in males

compared to females with an estimated ratio of 4:1. Despite a diverse range of symptoms reported for ASD, it is mainly characterized by three core features: 1) social interaction and, 2) communication impairments; 3) restricted and repetitive behaviors. A broad and divergent array of repetitive behaviors has been reported in individuals with ASD including stereotypies, rituals, compulsions, obsessions, and self-injures. [27, 23] Most ASD patients exhibit sleep disorders, either finding it difficult to fall asleep and/or experiencing frequent nocturnal awakenings which makes them vulnerable to night-time light and other factors that lead to circadian disruption. [44]

Because *in vivo* and biochemical experimentation on human patients with ASD is not feasible, animal models are used to study ASD, with the most common being mouse models due to genetic similarities to humans, the ease of genetic manipulation, and these rodent species being available. [23]

1.2.1 Mouse Models of Autism

Various ASD mouse models have been generated that contain genetic mutations found in human patients. These transgenic mice display various ASD phenotypes including diminished learning, impaired social behavior, and repetitive behaviors. [23] Mutations in the Contactin-Associated Protein-like 2 (*CNTNAP2*) gene are among the common risk genes associated with ASD. The *CNTNAP2* gene codes for the Contactin-ASsociated Protein-like 2 (CASPR2), a neural transmembrane scaffolding protein involved in neural development. Its absence contributes to aberrant autistic phenotypes. Mouse models that carry a null mutation in the *CNTNAP2* gene manifest several phenotypic characteristics of ASD such as social deficits, communication impairments, and increased repetitive and hyperactive behaviors. [48] Additionally, atypical neuronal migration, reduced number of cortical inhibitory interneurons, and abnormal cortical connectivity have been reported in *Cntnap2* mutant mice. [15, 14]

1.2.1.1 Repetitive behavior in CNTNAP2 knock-out (KO) mice

ASD mouse models in general display several stereotyped repetitive behaviors such as self-grooming, jumping, circling, and marble burying. Self-grooming behavior in mice is defined as scratching and brushing hair with forelimbs for a few seconds to minutes. However, when repeated more frequently and with a longer duration, self-grooming behavior can be classified as a repetitive behavior. Excessive self-grooming has been reported in *Cntnap2* Knockout (KO) mice, making this model a useful target for pharmaceutical research and a tool to understand and investigate the underlying mechanism of ASD aberrant behaviors. [23, 32] Studies have revealed that treating *Cntnap2* KO mice with risperidone, reduced their repetitive self-grooming behavior. [32]

1.2.2 Association of the basolateral amygdala (BLA) with stereotyped repetitive behavior in ASD

While the exact mechanisms underlying repetitive behavior in ASD remain unknown, several studies have shown that repetitive behavior is notably associated with the amygdala and the cerebral cortex. [38, 1, 13] Studies conducted on the development of the amygdala have reported an overgrowth of this brain region in children later diagnosed with ASD and increased amygdala volume in adolescents with ASD. [38, 1] It has been suggested that this increased volume may be due to underlying alterations in cellular density. Additionally, studies reported an association between enlarged amygdala central nuclei and increased repetitive behaviors in children and adolescents with ASD. [38] This finding suggests that the amygdala may be a candidate brain region involved in the self-grooming of ASD mouse models including the *Cntnap2* KO. Prior work that investigated the activity of neuronal populations in the amygdala of mouse models of ASD revealed that the glutamatergic cell population of the BLA plays an important role in driving repetitive behaviors. [46, 13]

1.2.3 Association of the prefrontal cortex (PFC) with stereotyped repetitive behavior in ASD

Previous studies have shown stimulation of PFC projections to the ventral tegmental area (VTA) as systemic application of phencyclidine (PCP), an NMDA receptor antagonist, evoked stereotyped self-grooming in rodents. Conversely, inhibition of the PFC-VTA glutamatergic projections alleviated repetitive behaviors. [13] PFC projections to the substantia nigra pars compacta (SNc) activate dopamine release in the striatum which could promote repetitive motor behavior in mice through two mechanisms: 1) dopamine activates the direct pathway in the basal ganglia by binding to D1 receptor, which results in increased movement; 2) dopamine inhibits the indirect pathway in the basal ganglia by acting on D2 receptor, which induces locomotion. Moreover, the application of Risperidone, a D2 receptor blocker, mitigated repetitive self-grooming behavior, in the *Cntnap2* mutants. These findings provide supporting evidence that the PFC may modulate repetitive behavior in *Cntnap2* KO mice. [23, 13]

1.3 Contribution of circadian disruption to ASD

Circadian misalignment may actively contribute to the development and mediate the severity of symptoms in individuals with ASD. Therefore, interest is growing in understanding the role of circadian disruption on the symptomatic profile of ASD. In a study of parental reports of autistic children, it was found that sleep deprivation is correlated with deficits in social interaction, elevated aggressiveness and anxiety, mood variation, hyperactivity, heightened sensitivity to changes in the environment, attention deficits, and increased incidence of repetitive behavior. Additionally, fragmented sleep was found to be associated with increases in restricted or repetitive behavior in ASD children. [22]

1.3.1 Environmental disruption of circadian rhythm increases repetitive behavior in ASD mouse model

A study by Fang et.al., demonstrated that disruption of circadian rhythms by ambient light during neurodevelopment leads to increased repetitive behaviors in adult mice. This study that was conducted on, a short day (SD) mouse model (8 h/8 h light/dark (LD) cycle was from embryonic day 1 to postnatal day 42), reported increased total grooming times and longer bout duration in SD mice compared with the control in a spontaneous self-grooming test. [10] Another study by Wang et.al,. found a link between circadian-disrupting environment and aggravated repetitive behavior in the *Cntnap2* KO mouse model of ASD. This study demonstrated that 2 weeks of exposure to dim light at night (DLaN, at 5-10 lx) causes selective vulnerability to the impact of DLaN on repetitive grooming behavior in Cntnap2 KO mutants and wild-type (WT) controls. [44]

These findings provide experimental evidence that links the environmental disruption of circadian rhythms to the pathogenesis of ASD.

1.3.2 Circadian disruption by night illumination alters the innate immune functions

The growing prevalence of night shift work and escalated use of electronic devices at night has become the main source of exposure to light at night. Increasing evidence has demonstrated that increased exposure to nighttime illumination impairs an organism's innate immune responses. Studies have reported elevated microglia pro-inflammatory cytokine expression (TNF and IL-6) following lipopolysaccharide (LPS) administration in male Swiss Webster mice housed in 5 lx artificial light at night (ALAN)for 4 weeks. Furthermore, housing male Swiss Webster mice in 5 lx ALAN for 7 days following cardiac arrest resulted in an increase in proinflammatory cytokine. [43]

Similarly, repetitive grooming behavior was reported to be proportional to the levels of

INF-γ, IL-6, IL-13, and CCL-11 in *Cntnap2* KO mice treated under DlaN. Preliminary data shows a significant increase in the levels of IFN-γ and IL-6 in the PFC of these mutants. Additionally, data suggests that carprofen treatment blocks DLaN-inducing an increase in the levels of IFN-γ and IL-6 in the PFC in mutant mice. [45]

Together, this data suggests that environmental perturbation drives inflammatory changes in mouse models of autism, and these immune changes are associated with the behavioral consequences of circadian disruption by night-time light exposure.

1.3.3 Microglia activation mediates circadian rhythm disruption

Microglia are the resident immune cells in the CNS with phagocytic capacity. It's been shown that with insult, injury, or disease in the CNS, microglia become activated and secrete proinflammatory cytokines such as TNF-α, IL-6, and IL-1β in the brain, causing inflammation that can be detrimental to neurogenesis and synapses. [24, 28]

Recent studies suggest that microglial dysfunction may be involved in the pathogenesis of ASD through attenuated synaptic pruning which could cause impairment in the brain's excitatory/inhibitory (E/I) imbalance and serves as the underlying cause of several neurodevelopmental disorders, including ASD. It's been suggested that an increased ratio of E/I, is the leading cause for hallmark phenotypes in ASD, including fundamental impairments in social interaction and repetitive behaviors. [24, 26] However, it is still unclear whether microglia fail to detect less active synapses, resulting in the excess number of excitatory synapses, or microglia are over-activated resulting in selective pruning of inhibitory synapses in the ASD brain. [24] **(Fig. 1.3)**

A previous study on male Swiss Webster mice revealed that 4 weeks of exposure to dim light at night (DLaN) induces microglia pro-inflammatory cytokine expression and leads to an elevation in ionized calcium-binding adaptor molecule 1 (Iba1) immunoreactivity, a marker for microglial activation following LPS administration. [12, 43]

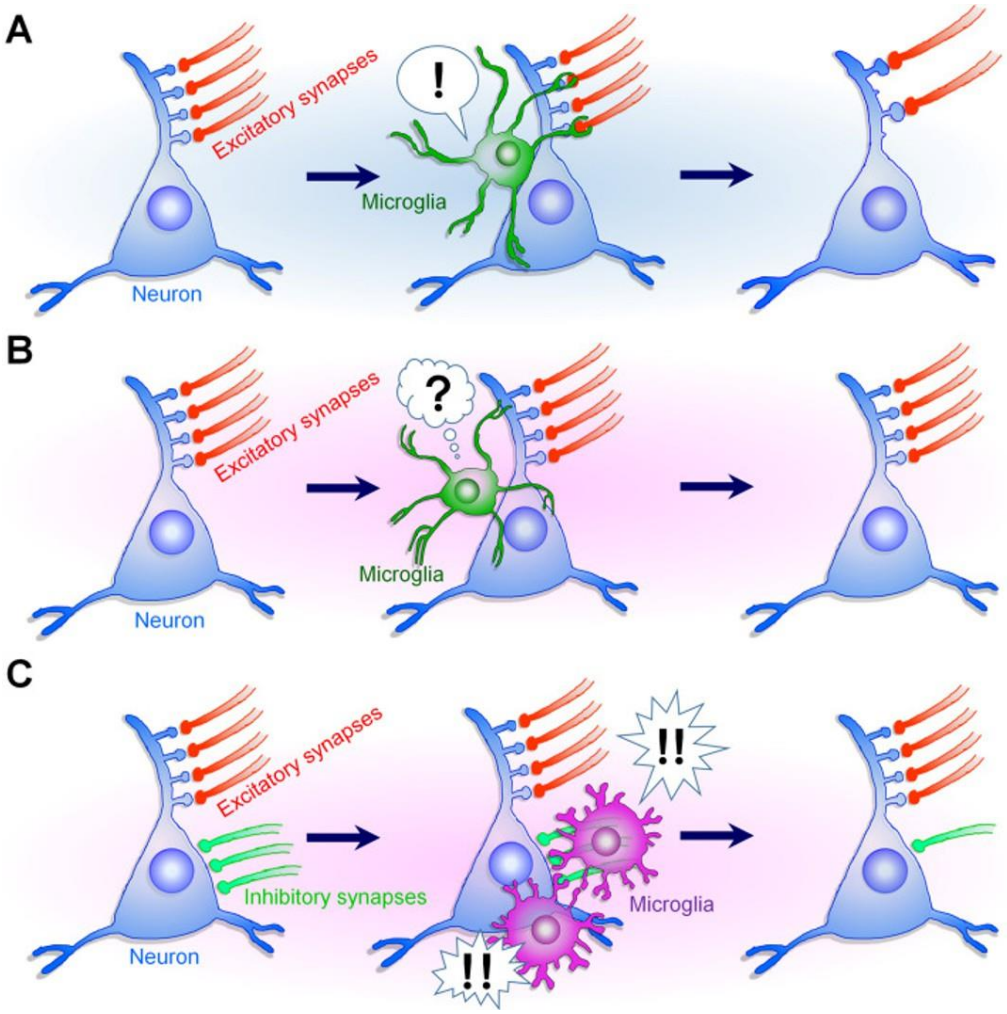

Figure 1.3: Schematic diagrams showing the possible involvement of microglia in E/I imbalance in ASD. (A) An excess number of immature excitatory synapses are first formed. Secondly, inappropriate and/or less active synapses are pruned by microglia. Finally, strong mature synapses are maintained. (B) In the ASD brain, microglia may fail to detect inappropriate or less active synapses, resulting in the maintenance of an excess number of immature and mature excitatory synapses. (C) In the ASD brain, microglia may be over-activated to selectively prune inhibitory synapses.

Evidence suggests that microglia are activated in various brain regions, including the PFC, in some ASD patients. [24] Preliminary data in our lab unveiled an elevation in IL-6 level and a selective increase in microglia proliferation and hyper-ramification changes in the PFC region of *Cntnap2* KO mice brain treated under DLaN. Moreover, the administration of the nonsteroidal anti-inflammatory drug, carprofen, which blocks COX-2 signaling, effectively counteracted the negative impacts of DLaN on grooming behavior in mutant mice. [45] These results provide supporting evidence about the possible role of microglia-mediated neuroinflammation in DLaN-driven changes in *Cntnap2* KO mice and the pathogenesis of ASD.

1.4 Thesis hypothesis

Strong evidence points to an involvement of the BLA in aberrant behaviors in rodents. [11] Prior work reported a DLaN-driven increase in cFos expression in the glutamatergic neuron in the BLA of *Cntnap2* KO mice raising the possibility activation of the glutamatergic neuron population in the BLA may contribute to the grooming behavior. [46] Additionally, previous studies implicated a dysfunctional prefrontal cortex (PFC) in ASD. [47, 4] Our preliminary data suggests changes in microglia density and morphology in the PFC of *Cntnap2* KO mice highlighting the possible microglia involvement in mediating DLaN-driven changes in this brain region. [45]

Considering that DLaN seems to elicit an increase in the number of microglia along with changes in morphology in the PFC, I sought to further investigate the role of microglia in mediating the effects of DLaN in both PFC and BLA, brain regions linked to repetitive behavior. Therefore, I hypothesized that exposure to DLaN may trigger an inflammatory response in the BLA and PFC regions and *Cntnap2* KO mice will be more sensitive to this effect compared to WT mice.

CHAPTER 2

Materials and Methods

2.1 Animals

All animal procedures were performed in accordance with the UCLA Animal Care Committee's regulations. Seventy-five-day-old male wild-type (WT) (C57BL/6J; strain: 000664) and *Cntnap2* knockout (strain: 017482) mice were purchased from Jackson Laboratory.

2.2 Housing and lighting conditions

Upon arrival, animals were single-housed in light-tight, temperature and humidity-controlled cabinets with free access to food and water and entrained for two weeks to a normal 12:12 hr light:dark (LD) cycle. Light intensity at ZT 0 (light-on) was 300 lx (as measured at the base of the cage and 0 lx at ZT 12 (light-off). Following the entrainment phase, mice were randomly assigned to one of two photic environments for two weeks: 1) 4 WT and 4 *Cntnap2* mice were held in the normal LD environment, while 2) the remaining mice (4 WT and 4 *Cntnap2*) were exposed to dim light at night (DLaN 5lx) during the dark phase. The experimental design is depicted in **Fig. 2.1.**

2.3 Immunohistochemistry

At the end of the 2-weeks, mice were anesthetized via inhalation of isoflurane (32%) at ZT 18 and transcardially perfused with ice-cold 1X phosphate-buffered saline (PBS, 0.1 M, pH

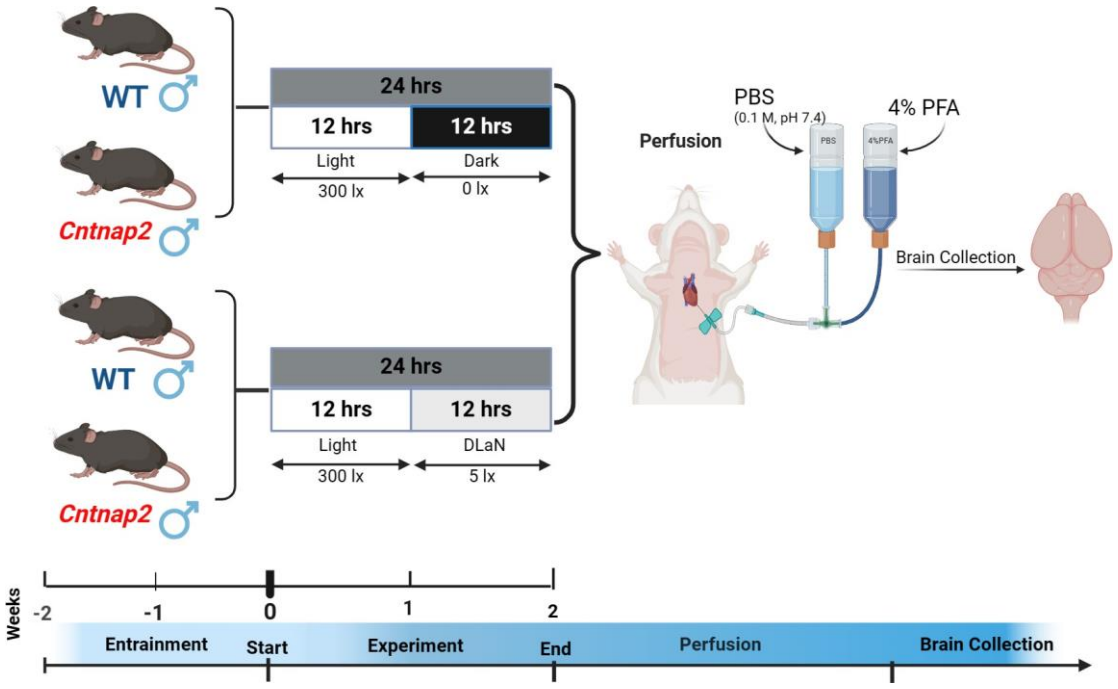

Figure 2.1: The Experimental Design. WT and *Cntnap2* KO mice were held under regular Light/Dark (LD; 300 lx) or exposed to DLaN (5 lx) for two weeks after which they were purfused with 4% PFA and their brains collected.

7.4) followed by 4% paraformaldehyde (PFA) solution in 1×PBS. The brains were rapidly dissected out and postfixed in 4% PFA overnight at $4°^{C}$, then transferred to a 15% sucrose solution for cryopreservation and stored at $4°^{C}$. Coronal brain sections (50 µM thickness) containing the brain regions of interest (PFC and BLA) were collected sequentially on a cryostat (Leica, Buffalo Grove, IL). Free-floating coronal sections (3 sections/animal) were paired along the rostal-caudal axis and then blocked for 1 hr at room temperature with gentle shacking in carrier solution (1% BSA, 0.3% Triton X-100, 1X PBS) containing 10% normal donkey serum and then incubated overnight at $4°^{C}$ with a rabbit polyclonal antibody against Iba1 (1:1000, FUJIFILM Wako Chemicals U.S.A. Corporation, Richmond, VA), followed by a Cy3-conjugated donkey-anti-rabbit secondary antibody (Jackson Im-

munoResearch Laboratories, Bar Harbor, ME). After washing, sections were mounted and coverslips were applied with Vectashield mounting medium containing DAPI (4′-6-diamidino-2- phenylindole; Vector Laboratories, Burlingame, CA). Sections were visualized on a Zeiss AxioImager M2 microscope (Zeiss, Thornwood NY) equipped with an AxioCam MRm and the ApoTome imaging system.

2.4 Imaging and Histological Analyses and Quantification

Images of both the left and right BLA and PFC were acquired from three coronal sections per animal with a 20X objective and the tile tool of the Zeiss Zen digital imaging software. These were used to determine the number of Iba1 positive cells and measure the staining relative intensity and distribution. The Paxinos mouse brain atlas was used to identify both the left and right BLA and medial PFC (anterior cingulate and prelimbic cortex) in each section and set the regions of interest (ROI) with the ROI tool of the NIH ImageJ software (https://imagej.net/software/fiji/) for further analyses. The Prelimbic cortex receives inputs from several areas including the BLA. Cell counting and quantifications were performed by three observers masked to the genotype and experimental groups.

2.4.1 Cell counting

Iba1 positive cells were counted with the auxilium of the cell counter plugin of the NIH ImageJ software within two ROIs for the left and right medial PFC (738.20 × 715.95 *μm*; 2288.99 × 2220.0 pixels) and three for the left and right BLA (436.02 × 154.8 *μm*; 1352 × 480 pixels) in 3 consecutive sections per animal. The counts from each ROIs per image were summed and the values from the left and right regions were averaged to obtain one value/section. The values from the 3 sections were averaged to obtain one value per animal and presented as the mean ± SEM of 4 animals per experimental group.

2.4.2 Iba1 relative intensity

The relative intensity of Iba1 staining in the BLA and medial PFC was quantified in 3 sections per animal by scanning densitometry using the NIH ImageJ software. Three ROIs of fixed-size (436.02 × 154.8 *μm*; 1352 × 480 pixels) were set and the relative integrated density (mean gray values x area of the ROI) and the raw intensity density (sum of intensity units in selection or sum of the values of each pixel within the ROI) measured in both the left and right BLA. The 3 values obtained for each side/image were averaged to obtain a single number per side, left or right BLA, and these were then averaged to obtain one value/section. The values from the 3 sections were finally averaged to obtain one value per animal. A single ROI (size 911.06 × 715.95 *μm*; 2824.99 × 22220.0 pixels) was used to measure the relative intensity in the left and right medial PFC. The values of integrated density and raw intensity density measured in 3 sections/animal, both left and right PFC, were averaged to obtain one value/animal and are presented as the mean ± SD of 4 animals per experimental group.

2.4.3 Measuring fluorescence intensity using profile plot

The distribution of the staining intensity was obtained for each left and right BLA or PFC separately in three consecutive slices/animal using the Profile Plot Analysis feature of Image J. A rectangular ROIs was set for the BLA (541.8 x 574.37 *μm*; 1680.0 × 1780.99 pixels) and for the medial PFC (911.06 × 715.95 *μm*; 2824.99 × 22220.0 pixels), and a column plot profile was generated whereby the x-axis represents the horizontal distance through the BLA or PFC (lateral to medial) and the y-axis represents the average pixel intensity per vertical line within the rectangular box. **(Fig. 2.2)** Subsequent processing of the resulting profiles was performed for the left and right BLA or PFC images separately. Then these were averaged to obtain one profile plot per animal. Data are shown as the average profile/genotype/experimental condition (LD or DLaN; n = 3-4 animals). A curve fitting line was over-imposed using the LOWESS (Locally Weighted Scatterplot Smoothing) regression

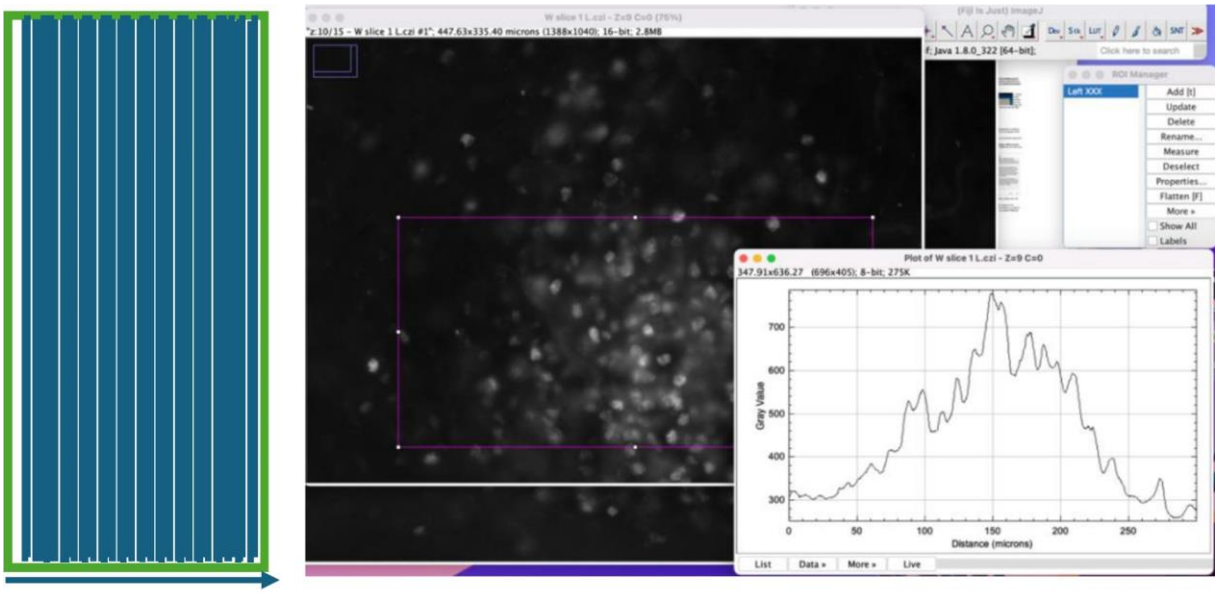

Figure 2.2: Schematic of the horizontal profile plot analysis. (A) Average intensity was measured along the vertical axis of rectangular ROI (parallel to the long side of the rectangle along the short side) with the aid of the horizontal profile plot analysis feature of the ImageJ software. (B) Profile plot of staining intensity and distribution within the ROI. Two-dimensional graph of the distribution of the relatively staining intensity within the ROI box. The x-axis represents the distance of pixels along and the y-axis is the pixel intensity.

analysis in Graph Pad Prism (version 10.2.3) to create a smooth line through the plot to visualize any potential trend in the data.

2.5 Statistics

All the statistical analysis of the data were performed using GraphPad Prism (version 10.2.3). Data are shown as the mean ± standard error of the mean (SEM) or standard deviation (SD) and were analyzed using a Two-Way analysis of variance (ANOVA) with genotype and light condition as factors. Differences were determined significant if $P < 0.05$.

CHAPTER 3

Results

Both the PFC and the BLA have been implicated in some of the aberrant behaviors observed in individuals with ASD, for instance, exacerbated repetitive behavior. In particular, the medial PFC receives inputs from several regions of the limbic systems linked to emotions and other functions, including the BLA. [19] DLaN was previously reported to elicit a greater increase in the levels of the marker for neuronal activation cFos in the BLA of Cntnap2 KO mice compared to WT, [46] along with increased repetitive behavior and decreased social interactions. [44, 46] Conversely, treatment with the anti-inflammatory drug, carprofen reversed the effects of DLaN on repetitive behavior measured as increased grooming time. [44] These findings suggest a possible role for inflammation and, thus, for microglia, the immune resident cells of the central nervous system, in mediating the effects of DLaN. Hence, I investigated whether exposure for two weeks to DLaN would have an impact on the number of microglia cells as well as on the expression levels of the microglia marker, Iba1.

Unpublished findings from our lab [45] showed an increase in the number of Iba1-positive cells in the medial PFC of *Cntnap2* KO mutants under DLaN. In addition, Sholl analysis identified differences in the number of processes in microglia in the mutants exposed to DLaN. Significant effects of genotype ($F(1,259) = 48.64$, $P < 0.001$), treatment ($F(1,259) = 16.88$, $P < 0.001$), and the radius ($F(1,259) = 30.71$, $P < 0.001$) were identified by three-way ANOVA, while the diameter, area, and perimeter of the cell somata were unaltered. These findings point to subtle cytomorphological changes occurring in microglia, in particular, DLaN exposure appears to trigger increased ramification in these cells as reported for other

mild chronic stress in the PFC. [21, 20]

3.1 Effects of DLaN exposure on microglia cells in the BLA of WT and *Cntnap2* KO mice

Encouraged by these unpublished findings from our lab, I, first, sought to determine if exposure to DLaN for two weeks would elicit changes in the number of Iba1 immunopositive cells in the BLA region. As shown in **Figure 3.1**, DLaN triggered a modest increase (15%) in the number of Iba1 positive cells in the BLA of *Cntnap2* KO mice when compared to mutants or WT held in LD condition. No changes were observed in the WT mice exposed to this stressor.

Next, I measured the integrated density and the raw intensity density of Iba1 staining in the BLA of WT and Cntnap2 mice exposed for two weeks to DLaN or held in LD. Iba1 expression was affected by DLaN in the BLA region of both genotypes, with the mutants showing a greater decrease (25%) in the expression of this marker compared to the WT (16%) or to the animals held on a regular LD cycle **(Fig. 3.2)**. A significant effect of the light condition, but not of genotype or the interaction between the two variables, was identified by two-way ANOVA ($F_{(1,12)}$=4.842; P=0.0481). This data suggests that DLaN exposure seems to have an impact on microglia in the BLA region.

To further characterize the changes observed in Iba1 immunoreactivity in the BLA of the WT and mutants after exposure to DLaN, I used the profile plot feature of ImageJ to identify possible changes in the staining distribution. This densitometric analysis confirmed the decreased immunoreactivity of Iba1 in the WT and mutants exposed to DLaN without changes in the staining distribution **(Fig 3.3 A** & **B)**. No particular trend was observed in the curves of any of the groups or between genotypes. These data suggest that DLaN exposure seems to have an effect on microglia in the BLA with the mutants being more impacted than WT mice.

3.2 Effects of DlaN exposure on microglia cells in the medial PFC of WT and *Cntnap2* KO mice

To further investigate the possible involvement of microglia cells in mediating the effects of DLaN, I determined if the light treatment induces changes in the integrated intensity and raw intensity density of Iba 1 staining in the medial PFC. No significant differences were observed between genotypes or lighting environment **(Fig. 3.4 A** & **B)**, although, a modest increase in the expression of Iba1 was observed in the mutants exposed to DLaN.

Furthermore, densitometric analysis of the distribution of Iba1 immunostaining revealed upregulated expression of this marker in both WT and Cntnap2 KO exposed to DLaN **(Fig 3.5 A** & **B)**, confirming the previous (unpublished) results. A qualitatively greater noise and amplitude in the signal could be appreciated in both WT and mutants exposed to DLaN **(Fig 3.5 A** & **B)**. Again, the fitted line did not show a particular trend, albeit a flatter fitted curves was displayed by the animals held in LD. These findings support the possibility of microglia playing a role in mediating DLaN effects and suggest that DLaN might have a greater effect on the medial PFC. Still, it remains to clarify whether or not these effects are genotype-specific.

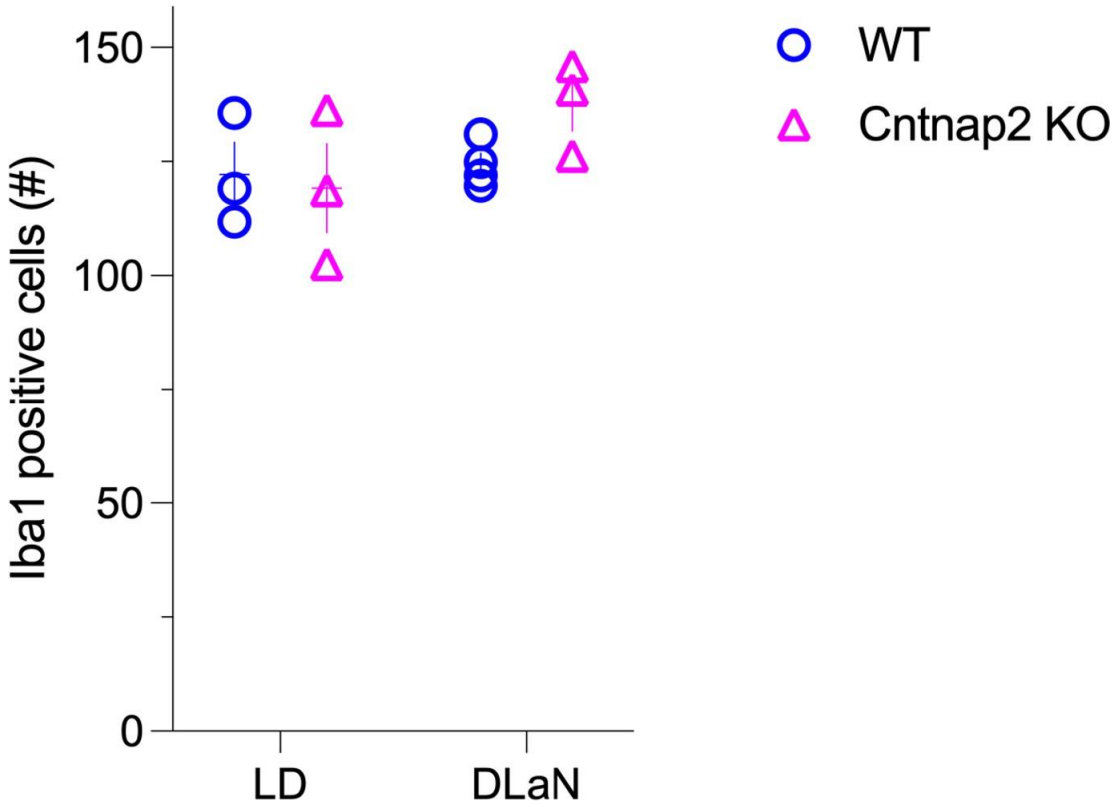

Figure 3.1: DLaN evoked changes in the number of Iba1+ cells in the BLA. A modest increase in the number of Iba1+ microglia was observed in the BLA of Cntnap2 KO mice. Two-way ANOVA analysis revealed no significant effects of genotype, photic environment, or their interaction. The graph represents the means ± SEM of 3-4 animals per genotype.

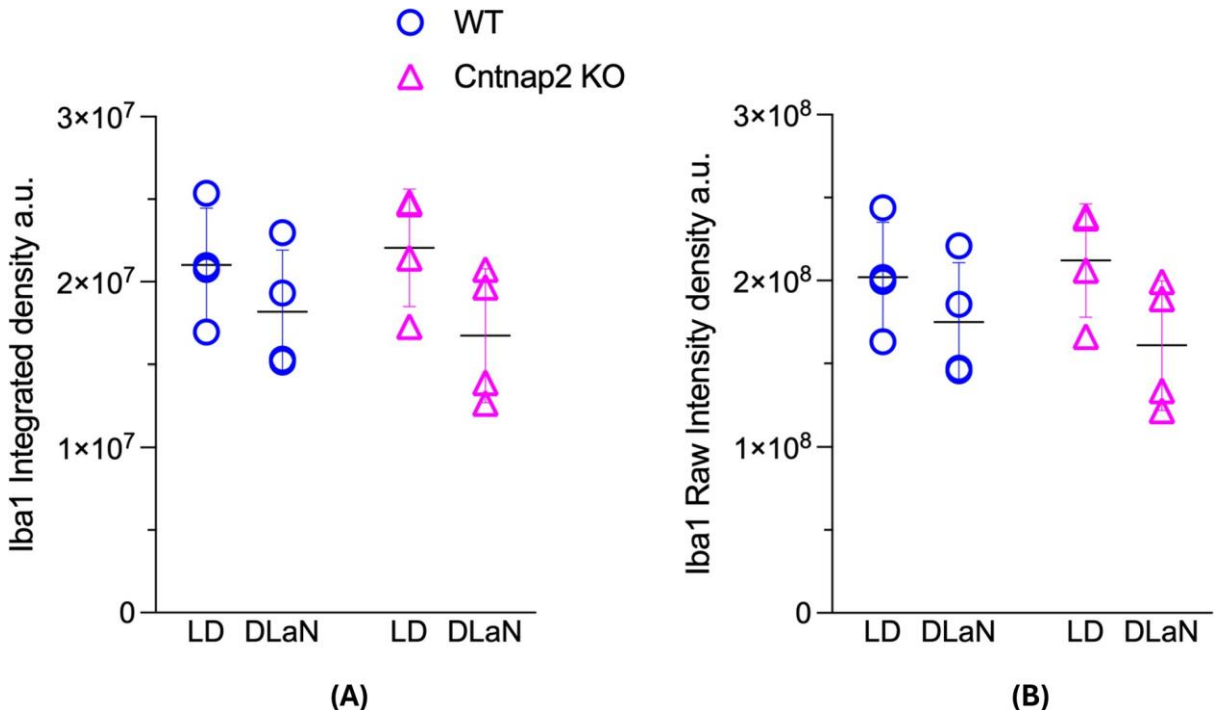

Figure 3.2: Altered expression of Iba1 in the BLA of WT and Cntnap2 KO mice exposed to DLaN. Both the WT and the mutants display a decrease in the intensity of Iba1 immunoreactivity. The Integrated Density (A) and Raw Intensity Density (B) were measured in Iba1-stained sections (3 sections/animal) containing both the left and right BLA. These can be defined as the "mean gray values x area of the ROI" and the "sum of intensity units in selection or sum of the values of each pixel within the ROI", respectively. The values from the left and right BLA sections were averaged to obtain one value per animal. The graph represents the mean ± SEM of 3-4 animals per genotype. (A, B) A significant effect of light was found by two-way ANOVA (5 lx) condition ($F_{(1,12)}$)=4.842; P=0.0481).

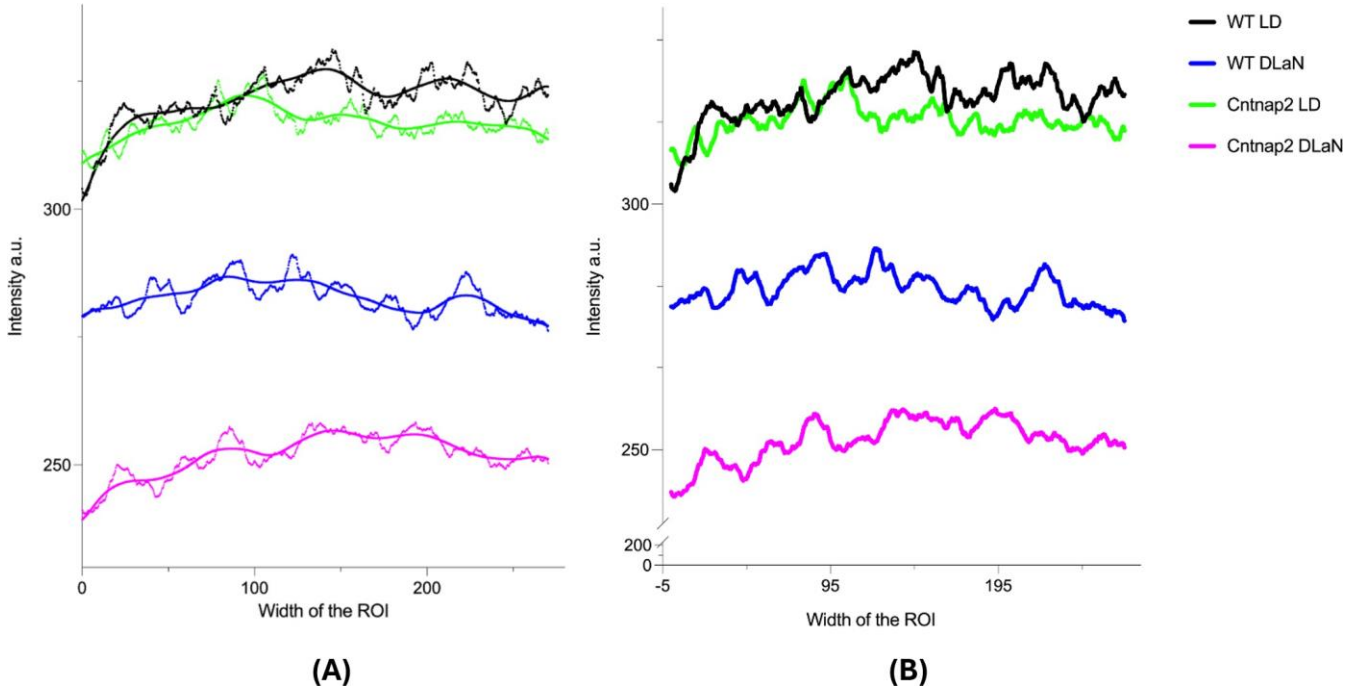

Figure 3.3: DLaN decreased Iba1 intensity in the BLA of WT and *Cntnap2* KO mice. (A, B) Densitometric analysis of Iba1 staining in the BLA region of WT and *Cntnap2* KO mice held in LD or exposed to DLaN (5 lx) revealed a marked decrease in the expression of this marker for microglia in the mutants exposed to DLaN without changes in the distribution of the staining. The relative intensity of Iba1-stained sections was measured using a rectangular ROI box positioned within the BLA and the profile plot feature of Image J. Values from the left and right BLA (3 sections/animal) were aligned and averaged to obtain one value/animal. The traces represent the mean of four animals. (A) A curve fitting line was superimposed using the LOWESS (Locally Weighted Scatterplot Smoothing) regression analysis in Graph Pad (Prism version 10.2.3) to create a smooth line through the plot to visualize any potential trend in the data.

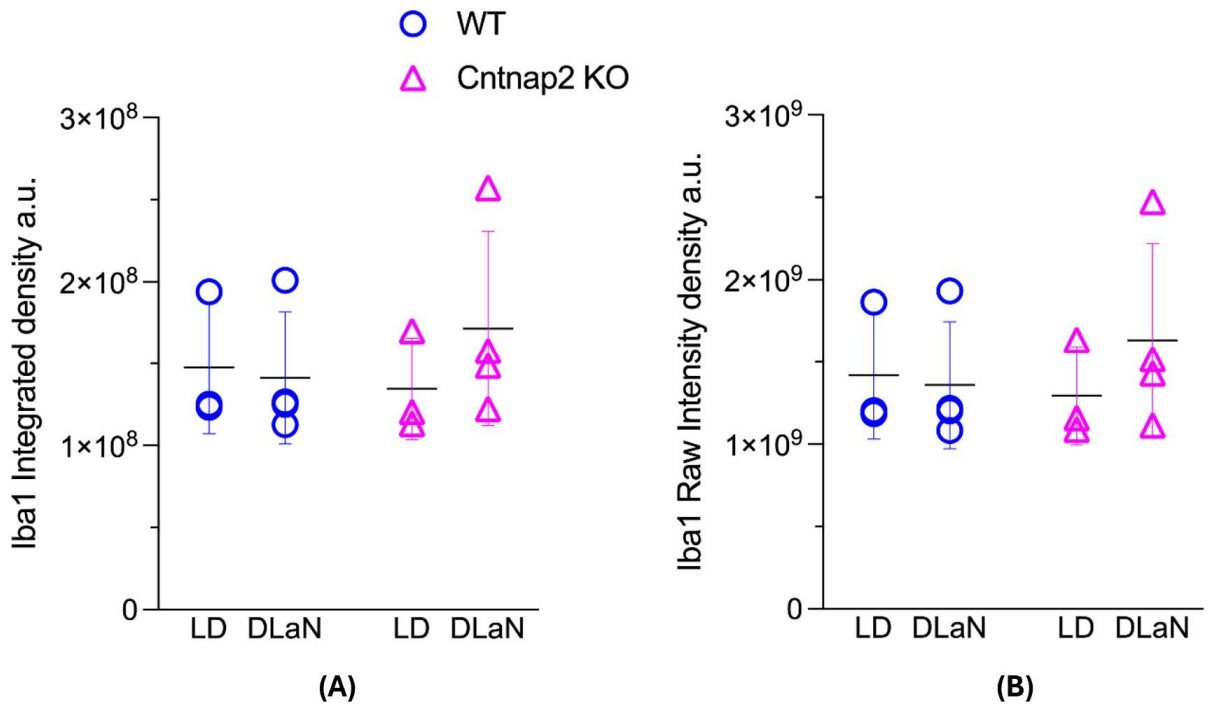

Figure 3.4: Unaltered expression of Iba1 in the medial PFC of WT and Cntnap2 KO mice exposed to DLaN. The mutants exposed to DLaN displayed a modest increase in Iba 1 intensity. The Integrated Density (A) and Raw Intensity Density (B) were measured in Iba1-stained sections (3 sections/animal) containing both the left and right PFC. These can be defined as the "mean gray values x area of the ROI" and the "sum of intensity units in selection or sum of the values of each pixel within the ROI", respectively. The values from the left and right PFC sections were averaged to obtain one value per animal. The graph represents the mean ± SEM of 4 animals per genotype.

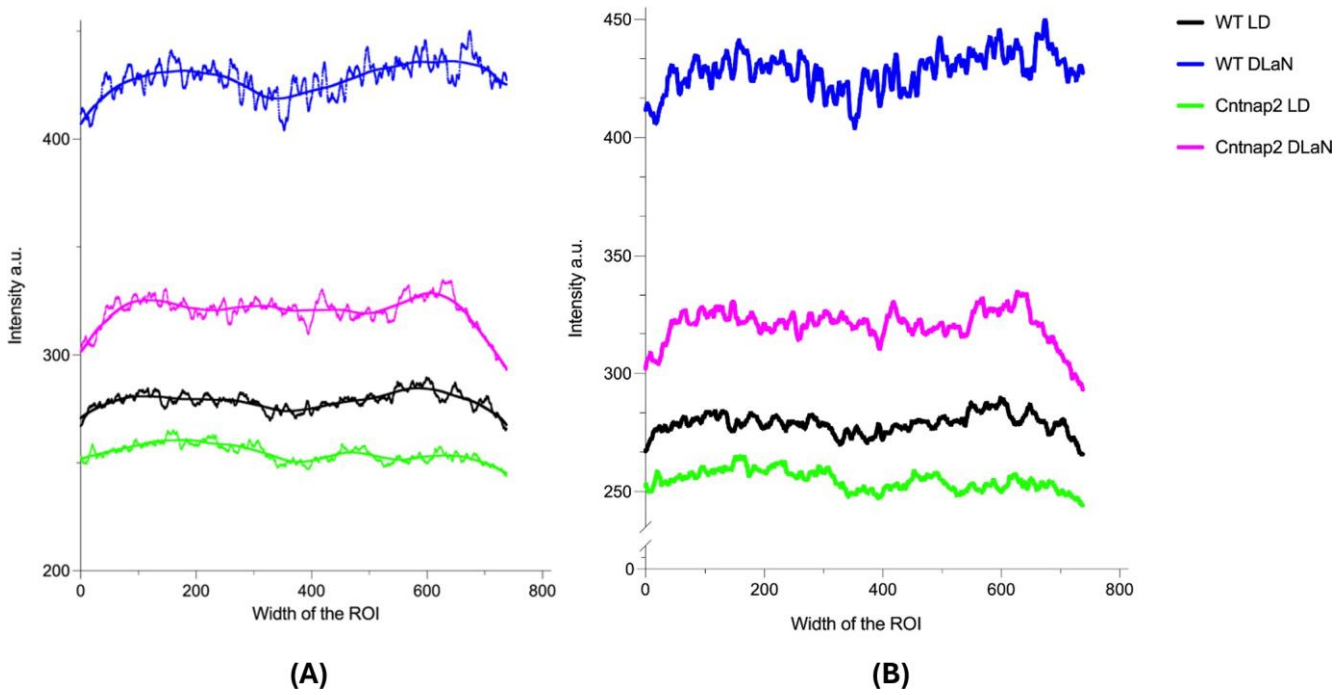

Figure 3.5: DLaN increased Iba1 intensity in the medial PFC of WT and Cntnap2 KO mice. (A, B) Densitometric analysis of Iba1 staining in the medial PFC of WT and Cntnap2 KO mice held in LD or exposed to DLaN (5 lx) revealed a marked increase in the expression of this marker for microglia in the WT and mutants exposed to DLaN. The relative intensity of Iba1-stained sections was measured in the medial PFC of both genotypes using one ROI and the profile plot feature of Image J. Values from the left and right PFC (3 sections/animal) were aligned and averaged to obtain one value/animal. The traces represent the mean of three-four animals. (A) A curve fitting line was over imposed using the LOWESS (Locally Weighted Scatterplot Smoothing) regression analysis in Graph Pad (Prism version 10.2.3) to create a smooth line through the plot to visualize any potential trend in the data.

CHAPTER 4

Discussion

My thesis study evaluated the possible contribution of microglia, the resident immune cells of the CNS, in mediating the effects of DLaN in the Cntnap2 KO mouse model of ASD. I found that DLaN exposure alters Iba1 immunoreactivity in the BLA and PFC, as well as Iba1+ cell number in the BLA of WT and mutant mice. I also found that alterations in Iba 1 positive microglia in the BLA region triggered by dim light are not genotype-specific as both WT and mutants were affected and finally the mutants did not seem to be more sensitive to the effects of DLaN compared to WT. Furthermore, my results show a slightly increased number of Iba1+ cells in the BLA of *Cntnap*2 KO mice compared to the other experimental groups which is inconsistent with the results from the intensity analysis.

In the DLaN condition (5 lx) my findings are in agreement with the preliminary data that suggests this treatment may trigger an inflammatory response in the PFC by inducing a change in the number and morphology of Iba+ microglia. My results from the intensity profile of Iba1+ immunoreactivity in the PFC under the DLaN condition are also in agreement with the evidence provided by a recent study that revealed increased microglial density in a brain-region-specific manner in the C58/J mouse model of idiopathic autism, particularly in the PFC and hippocampus. [9] However, my work is at variance with the preliminary results as the mutant mice showed a modest response in the medial PFC in comparison to WT. [45]

In previous work, microglial activation was implicated in mediating emotional learning in ASD post-mortem brains. [30]. In an animal model of ASD carrying a duplication of the

human chromosome 15q11-q13, microglial alterations in the BLA during early development were correlated with anxiety-related behavior in adolescence. [39] In addition, previous work from our lab examined cFos immunoreactivity in brain regions implicated in the control of repetitive behavior, such as the BLA, and in areas known to receive light information from the ipRGC, such as the peri-Habenula area (pHb) in WT and *Cntnap2* KO mice under LD or DLaN. Both WT and mutant mice exposed for 2 weeks to a short-λ enriched DLaN displayed a significantly increased number of cFos positive cells in both the BLA and pHb compared to mice held on a standard LD condition.[46]. All this evidence points to a role for the BLA in some of the aberrant behavior observed in ASD such as repetitive behavior, and suggests that DLaN may exacerbate repetitive behavior in mice by affecting microglia function in this nucleus. However, my findings are inconsistent with these studies as Iba1 expression was not impacted by exposure to DLaN in the BLA region of both genotypes, with the mutants showing a 25% decrease in the expression of this marker compared to 16 % in the WT or to the animal held under LD condition.

There are a number of possible mechanisms by which increased inflammation may contribute to some if not all the phenotypes of ASD. For example, a study on the role of the peripheral immune molecules on ASD behavior in the BTBR mouse model of ASD showed an increase in repetitive grooming behavior in C57 mice that received bone marrow from BTBR donors. These data provide supporting evidence for a causal relationship between the peripheral immune system and repetitive behavior in preclinical models. [37] Microglia plays several key roles during development, among others is involved in synaptic pruning. Synapse formation, pruning, and maturation are fundamental for the development of proper excitatory versus inhibitory (E/I) neurotransmission balance in the brain, and microglia are highly involved in it. In individuals with ASD, an E/I imbalance, especially an increased ratio of E/I, has been proposed as a possible leading cause for classical hallmark phenotypes in ASD, including repetitive behaviors. [35] Studies on disorders with behavioral phenotypes similar to autism spectrum disorder (ASD) such as mouse models of obsessive-compulsive disorder

and Rett syndrome suggested that attenuated or excessive synaptic pruning by microglia could impair the E/I balance in the CNS. [6, 8] Impairment of the GABAergic inhibitory neurotransmission has been observed in some animal models and linked to poor social be-behavior. For instance, a significant reduction in the frequency of spontaneous inhibitory postsynaptic currents (IPSCs) compared to a substantial increase in the frequency of spontaneous excitatory postsynaptic currents (EPSCs) has been shown in the hippocampal CA1 pyramidal neurons of the BTBR mouse model. [16] Importantly, increasing the GABAergic neurotransmission using a positive allosteric modulator, such as the benzodiazepine clonazepam, improved the animals' behavior, including social interactions, repetitive behavior, and spatial learning. Previous studies suggested that the complement proteins C1q and C3, highly localized to immature synapses, may tag unwanted synapses for removal by phagoytic macrophages via specific complement receptors. Furthermore, less active synapses might also be tagged by the C3 protein and then detected and pruned by microglia that express the complement receptor 3 (CR3/cd11b). [40, 36] Hence, it could be speculated that elevated levels of complement proteins in the ASD brain may promote synaptic pruning by microglia. Alternatively, increased complement proteins could cover the specific localization of complement proteins on less active synapses, preventing the pruning of unwanted synapses by microglia. Future studies are required to identify the underlying mechanisms involved in the complement-microglia interactions that might impair the E/I balance as well as why microglia would preferentially engulf inhibitory synapses.

Prior work reported elevated short-λ DLaN-driven cFos expression in male WT and *Cntnap2* KO mice in the peri-habenular nucleus (pHb). [46] This area has been shown to mediate some of the effects of light on mood and learning hence, the pHb could be also involved in mediating some of the effects of DLaN in BTBR mice, a positive correlation was found between the diminished level of response to the presentation of social stimuli and blunted c-Fos immunopositivity in the lateral habenula (LHb) [18] Future studies should examine the effects of DLaN on Iba1 immunoreactivity in the pHb as well as the lateral and medial habenula in *Cntnap2* KO.

In conclusion, my thesis study provides pieces of evidence supporting the hypothesis that microglia may mediate the deleterious effects of circadian rhythm disruption by nighttime exposure to light in the *Cntnap2* mouse model of autism. DLaN treatment evoked a mild increase in the number of Iba1+ cells in the BLA region (Figure 3.1) of *Cntnap2* genotypes KO mice and increased microglia immunoreactivity in the PFC region (Figure 3.5). In addition, alterations in microglia evoked by DLaN were not specific to mutants.

References

[1] Thomas A Avino et al. “Neuron numbers increase in the human amygdala from birth to adulthood, but not in autism”. In: *Proceedings of the National Academy of Sciences* 115.14 (2018), pp. 3710–3715.

[2] Frank Bellivier et al. “Sleep-and circadian rhythm–associated pathways as therapeutic targets in bipolar disorder”. In: *Expert opinion on therapeutic targets* 19.6 (2015), pp. 747–763.

[3] David M Berson, Felice A Dunn, and Motoharu Takao. “Phototransduction by retinal ganglion cells that set the circadian clock”. In: *Science* 295.5557 (2002), pp. 1070–1073.

[4] Lucy K Bicks et al. “Prefrontal cortex and social cognition in mouse and man”. In: *Frontiers in psychology* 6 (2015), p. 166005.

[5] Christine Blume, Corrado Garbazza, and Manuel Spitschan. “Effects of light on human circadian rhythms, sleep and mood”. In: *Somnologie* 23.3 (2019), p. 147.

[6] Shau-Kwaun Chen et al. “Hematopoietic origin of pathological grooming in Hoxb8 mutant mice”. In: *Cell* 141.5 (2010), pp. 775–785.

[7] Anne M Curtis et al. “Circadian clock proteins and immunity”. In: *Immunity* 40.2 (2014), pp. 178–186.

[8] N o ë l C Derecki et al. “Wild-type microglia arrest pathology in a mouse model of Rett syndrome”. In: *Nature* 484.7392 (2012), pp. 105–109.

[9] Juan F Duarte-Campos et al. “Changes in neuroinflammatory markers and microglial density in the hippocampus and prefrontal cortex of the C58/J mouse model of autism”. In: *European Journal of Neuroscience* 59.1 (2024), pp. 154–173.

[10] Kun Fang et al. “Disruption of circadian rhythms by ambient light during neurodevelopment leads to autistic-like molecular and behavioral alterations in adult mice”. In: *Cells* 10.12 (2021), p. 3314.

[11] Ada C Felix-Ortiz et al. “Bidirectional modulation of anxiety-related and social behaviors by amygdala projections to the medial prefrontal cortex”. In: *Neuroscience* 321 (2016), pp. 197–209.

[12] Laura K Fonken, Zachary M Weil, and Randy J Nelson. “Mice exposed to dim light at night exaggerate inflammatory responses to lipopolysaccharide”. In: *Brain, Behavior, and Immunity* 34 (2013), pp. 159–163.

[13] Tanya Gandhi and Charles C Lee. “Neural mechanisms underlying repetitive behaviors in rodent models of autism spectrum disorders”. In: *Frontiers in cellular neuroscience* 14 (2021), p. 592710.

[14] Tanya Gandhi et al. “Behavioral regulation by perineuronal nets in the prefrontal cortex of the CNTNAP2 mouse model of autism spectrum disorder”. In: *Frontiers in Behavioral Neuroscience* 17 (2023), p. 1114789.

[15] Tanya Gandhi et al. “Neuroanatomical Alterations in the CNTNAP2 Mouse Model of Autism Spectrum Disorder”. In: *Brain Sciences* 13.6 (2023), p. 891.

[16] Sung Han et al. “Enhancement of inhibitory neurotransmission by GABAA receptors having α2, 3-subunits ameliorates behavioral deficits in a mouse model of autism”. In: *Neuron* 81.6 (2014), pp. 1282–1289.

[17] Michael H Hastings, Elizabeth S Maywood, and Marco Brancaccio. “Generation of circadian rhythms in the suprachiasmatic nucleus”. In: *Nature Reviews Neuroscience* 19.8 (2018), pp. 453–469.

[18] Yuki Higuchi, Shun-ichi Tachigori, and Hiroyuki Arakawa. “Faded neural projection from the posterior bed nucleus of the stria terminalis to the lateral habenula contributes to social signaling deficit in male BTBR mice as a mouse model of autism”. In: *Psychoneuroendocrinology* 149 (2023), p. 106004.

[19] Busha Hika and Yasir Al Khalili. “Neuronatomy, prefrontal association cortex”. In: *StatPearls [Internet]*. StatPearls Publishing, 2023.

[20] Madeleine Hinwood et al. “Chronic stress induced remodeling of the prefrontal cortex: structural re-organization of microglia and the inhibitory effect of minocycline”. In: *Cerebral cortex* 23.8 (2013), pp. 1784–1797.

[21] Madeleine Hinwood et al. “Evidence that microglia mediate the neurobiological effects of chronic psychological stress on the medial prefrontal cortex”. In: *Cerebral cortex* 22.6 (2012), pp. 1442–1454.

[22] Ramanujam Karthikeyan et al. “Understanding the role of sleep and its disturbances in autism spectrum disorder”. In: *International Journal of Neuroscience* 130.10 (2020), pp. 1033–1046.

[23] Hyopil Kim, Chae-Seok Lim, and Bong-Kiun Kaang. “Neuronal mechanisms and circuits underlying repetitive behaviors in mouse models of autism spectrum disorder”. In: *Behavioral and Brain Functions* 12 (2016), pp. 1–13.

[24] Ryuta Koyama and Yuji Ikegaya. “Microglia in the pathogenesis of autism spectrum disorders”. In: *Neuroscience research* 100 (2015), pp. 1–5.

[25] Yannuo Li and Ioannis P Androulakis. “Light entrainment of the SCN circadian clock and implications for personalized alterations of corticosterone rhythms in shift work and jet lag”. In: *Scientific reports* 11.1 (2021), p. 17929.

[26] Xiaoli Liao et al. “Microglia mediated neuroinflammation in autism spectrum disorder”. In: *Journal of psychiatric research* 130 (2020), pp. 167–176.

[27] Catherine Lord et al. “Autism spectrum disorder”. In: *Nature reviews Disease primers* 6.1 (2020), pp. 1–23.

[28] Dongli Meng et al. “Microglia activation mediates circadian rhythm disruption-induced cognitive impairment in mice”. In: *Journal of neuroimmunology* 379 (2023), p. 578102.

[29] Ralph E Mistlberger. “Circadian regulation of sleep in mammals: role of the suprachiasmatic nucleus”. In: *Brain research reviews* 49.3 (2005), pp. 429–454.

[30] John T Morgan et al. “Stereological study of amygdala glial populations in adolescents and adults with autism spectrum disorder”. In: *PloS one* 9.10 (2014), e110356.

[31] Ketema N Paul, Talib B Saafir, and Gianluca Tosini. “The role of retinal photoreceptors in the regulation of circadian rhythms”. In: *Reviews in endocrine and metabolic disorders* 10 (2009), pp. 271–278.

[32] Olga Peñagarikano and Daniel H Geschwind. “What does CNTNAP2 reveal about autism spectrum disorder?” In: *Trends in molecular medicine* 18.3 (2012), pp. 156–163.

[33] Vallath Reghunandanan and Rajalaxmy Reghunandanan. “Neurotransmitters of the suprachiasmatic nuclei”. In: *Journal of circadian rhythms* 4.1 (2006), p. 2.

[34] Alan M. Rosenwasser and Fred W. Turek. “Chapter 34 - Physiology of the Mammalian Circadian System”. In: *Principles and Practice of Sleep Medicine (Fifth Edition)*. Ed. by Meir H. Kryger, Thomas Roth, and William C. Dement. Fifth Edition. Philadelphia: W.B. Saunders, 2011, pp. 390–401. isbn: 978-1-4160-6645-3.

[35] JLR Rubenstein and Michael M Merzenich. “Model of autism: increased ratio of excitation/inhibition in key neural systems”. In: *Genes, Brain and Behavior* 2.5 (2003), pp. 255–267.

[36] Dorothy P Schafer et al. “Microglia sculpt postnatal neural circuits in an activity and complement-dependent manner”. In: *Neuron* 74.4 (2012), pp. 691–705.

[37] Jared J Schwartzer et al. “C57BL/6J bone marrow transplant increases sociability in BTBR T+ Itpr3tf/J mice”. In: *Brain, behavior, and immunity* 59 (2017), pp. 55–61.

[38] Diane Seguin et al. “Amygdala subnuclei development in adolescents with autism spectrum disorder: Association with social communication and repetitive behaviors”. In: *Brain and Behavior* 11.8 (2021), e2299.

[39] Tomoko Shigemori et al. “Altered microglia in the amygdala are involved in anxiety-related behaviors of a copy number variation mouse model of autism”. In: *Journal of Nippon Medical School* 82.2 (2015), pp. 92–99.

[40] Beth Stevens et al. “The classical complement cascade mediates CNS synapse elimination”. In: *Cell* 131.6 (2007), pp. 1164–1178.

[41] Alana Taub et al. “Arginine vasopressin-containing neurons of the suprachiasmatic nucleus project to CSF”. In: *eneuro* 8.2 (2021).

[42] Martha Hotz Vitaterna, Joseph S Takahashi, and Fred W Turek. “Overview of circadian rhythms”. In: *Alcohol research & health* 25.2 (2001), p. 85.

[43] William H Walker et al. “Light at night disrupts biological clocks, calendars, and immune function”. In: *Seminars in immunopathology*. Springer. 2022, pp. 1–9.

[44] Huei Bin Wang et al. “Melatonin treatment of repetitive behavioral deficits in the Cntnap2 mouse model of autism spectrum disorder”. In: *Neurobiology of disease* 145 (2020), p. 105064.

[45] Huei-Bin Wang. *The Mechanisms Underlying Exacerbated Autistic Behavior Induced by the Circadian-disrupting Environment of Nightly Illumination*. University of California, Los Angeles, 2022.

[46] Huei-Bin Wang et al. “Long wavelength light reduces the negative consequences of dim light at night”. In: *Neurobiology of disease* 176 (2023), p. 105944.

[47] Ofer Yizhar. “Optogenetic insights into social behavior function”. In: *Biological psychiatry* 71.12 (2012), pp. 1075–1080.

[48] Peñagarikano Olga. “New therapeutic options for autism spectrum disorder: experimental evidence”. In: *Experimental neurobiology* 24.4 (2015), pp. 301.